EDGE ARTICLE

Check for updates

All publication charges for this article have been paid for by the Royal Society of Chemistry

C(sp³)–H cyanation by a formal copper(III) cyanide complex†

Jamey K. Bower,‡ Maxwell S. Reese,‡ Ilia M. Mazin, Lina M. Zarnitsa, Andrew D. Cypcar, Curtis E. Moore, Alexander Yu. Sokolov * and Shiyu Zhang *

High-valent metal oxo complexes are prototypical intermediates for the activation and hydroxylation of alkyl C–H bonds. Substituting the oxo ligand with other functional groups offers the opportunity for additional C–H functionalization beyond C–O bond formation. However, few species aside from metal oxo complexes have been reported to both activate and functionalize alkyl C–H bonds. We herein report the first example of an isolated copper(III) cyanide complex ($LCu^{III}CN$) and its C–H cyanation reactivity. We found that the redox potential (E_{ox}) of substrates, instead of C–H bond dissociation energy, is a key determinant of the rate of PCET, suggesting an oxidative asynchronous CPET or ETPT mechanism. Among substrates with the same BDEs, those with low redox potentials transfer H atoms up to a million-fold faster. Capitalizing on this mechanistic insight, we found that $LCu^{III}CN$ is highly selective for cyanation of amines, which is predisposed to oxidative asynchronous or stepwise transfer of H^+/e^-. Our study demonstrates that the asynchronous effect of PCET is an appealing tool for controlling the selectivity of C–H functionalization.
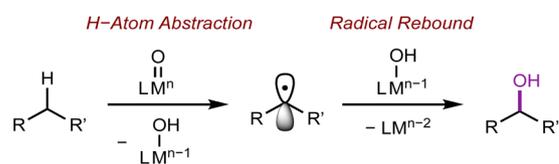
Introduction

Nature has evolved metalloenzymes that rapidly and selectively hydroxylate aliphatic C–H bonds under ambient conditions with earth-abundant metals.[1] The rate-limiting step of C–H hydroxylation – hydrogen atom abstraction (HAA) – is often mediated by high-valent metal-oxo intermediates (Scheme 1A).[2-4] The remarkable HAA ability of metal-oxo intermediates has motivated intense efforts to understand the factors that underpin the reactivity. A large body of experimental and theoretical studies were dedicated to investigating the movement of protons and electrons from C–H substrates to metal oxo complexes.[5,6] These studies have important implications in understanding the activation energies of HAA reactions, which can predominately trend with the driving force of proton transfer (PT, ΔG°_{PT}), electron transfer (ET, ΔG°_{ET}), or proton-coupled electron transfer (PCET, $\Delta G^{\circ}_{PCET} = \Delta G^{\circ}_{PT} + \Delta G^{\circ}_{ET}$).[7,8] While C–H bond cleavage is often considered as a synchronous PCET that is governed by bond dissociation free energy, recent studies by Anderson,[9] Borovik,[10,11] Tolman, Cramer,[12] Kojima,[13,14] and Fukuzumi[15] show that the basicity (pK_a) or redox potential (E°) of the C–H-activating metal complexes can also be the determining factor for C–H activation.
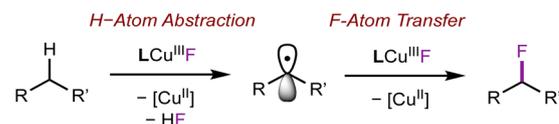
In addition to the successful demonstration of metal-oxo species for C–H activation and functionalization,[4,16-18] a variety of synthetic high-valent metal complexes carrying other functional groups M–FG, *e.g.*, OH, superoxo, carboxylate, halides, nitrite, and nitrate, have been shown to activate C–H bonds. The studies by Tolman,[12,19-23] McDonald,[24-28] us,[29] and others[30-32] have demonstrated that C–H activation can be achieved in the absence of the oxo ligand through mechanistically similar HAA/PCET processes
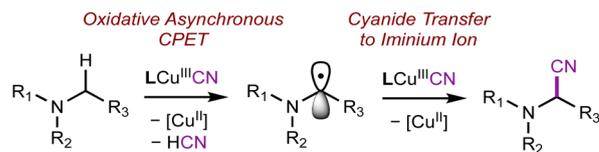
Department of Chemistry and Biochemistry, The Ohio State University, 100 W. 18th Ave, Columbus, OH, 43210, USA. E-mail: zhang.8941@osu.edu

‡ These authors contributed equally.

A. C–H hydroxylation via metal oxo-complexes

H–Atom Abstraction — *Radical Rebound*

B. Previous work: C–H fluorination via copper(III) fluoride

H–Atom Abstraction — *F–Atom Transfer*

C. This work: C–H cyanation of amines via copper(III) cyanide

Oxidative Asynchronous CPET — *Cyanide Transfer to Iminium Ion*

• first fully characterized copper(III) cyanide complex
• new mechanism for copper(II)/(III) C–H functionalization
• modular platform for C–H functionalization

Scheme 1

with M–FG. However, in contrast to metal oxo species, few M–FG complexes have been shown to subsequently functionalize the substrate following C–H activation.[23,29] Seminal research by Tolman[12,19–23] and McDonald[24–28] showed that pyridinedicarboxamide (**L**) Cu(III) and Ni(III) complexes can activate strong C–H bonds. Employing the same ligand **L**, we established that a copper(III) fluoride complex (**LCu^{III}F**) can perform sp^3 C–H fluorination by sequential HAA and fluorine atom transfer, similar to the mechanism of metal-oxo-mediated C–H functionalization (Scheme 1B).[29] The modularity of **L** is particularly attractive, as one could envision substituting fluorine with other desirable functional groups in C–H functionalization sequences.

Toward this end, we were motivated to investigate the reactivity of copper(III) cyanide complexes for C–H cyanation. Nitriles are particularly valuable synthetic motifs since the –C≡N group provides a handle to develop molecular complexity through further functional group manipulation.[33] For example, α-aminonitriles are a common motif in anti-tumor therapeutics and important synthetic precursors to 1,2-diamines and β-amino acids.[33] Recently, many copper-catalyzed cyanation reactions have been developed.[25–36] High-valent copper(III) cyanide complexes are often proposed as reactive intermediates in cyanation reactions, *e.g.*, cross-coupling,[34–36] radical-relay C–H cyanation,[37–42] or photoinduced cyanation.[43–45] The key C–CN bond formation steps are often proposed to involve reductive elimination from the organocopper(III) cyanide species. However, copper(III) cyanide intermediates are often too short-lived for isolation, preventing rigorous characterization and interrogation of their participation in key mechanistic steps.

Herein, we report the synthesis, characterization, and C–H cyanation reactivity of the first fully characterized formal copper(III) cyanide complex, **LCu^{III}CN** (Scheme 1C). Interestingly, while benzylic and allylic substrates (BDE ∼90 kcal mol^{-1}) are not amenable for C–H cyanation by **LCu^{III}CN**, trialkylamines with essentially the same C–H BDE (∼89–93 kcal mol^{-1})[46] readily undergo C–H cyanation in up to 90% yields. The contrasting reactivity of benzylic and α-amino C–H bonds with **LCu^{III}CN** was attributed to the large thermodynamic bias between ET and PT.[7]

Results and discussion

Synthesis, characterization, and electronic structure of a formal copper(III) cyanide complex

We first synthesized the copper(II) cyanide complex using a procedure analogous to previously reported copper(II) hydroxide and halide complexes.[19,29] Treatment of the copper(II) acetonitrile complex, **LCu^{II}MeCN**, with tetrabutylammonium cyanide (TBACN) affords the anionic copper(II) cyanide complex, [TBA]**LCu^{II}CN** in 94% yield. X-ray diffraction analysis of single crystals obtained from a THF/diethyl ether solution shows a square planar copper(II) center with a linear Cu–CN unit (Fig. 2A). The cyclic voltammogram (CV) of [TBA]**LCu^{II}CN** in CH$_2$Cl$_2$ exhibits a quasi-reversible redox couple at $E_{1/2} = 0.585$ V (*vs.* Ag/AgNO$_3$) (Fig. 1B), which is the highest among the **LCu$^{III/II}$** halide/pseudohalide series (F 0.395 V, Cl 0.458 V, Br 0.463 V in CH$_2$Cl$_2$).[29]

Having demonstrated the chemical reversibility of the formal copper(II)/(III) cyanide redox couple, we investigated the chemical
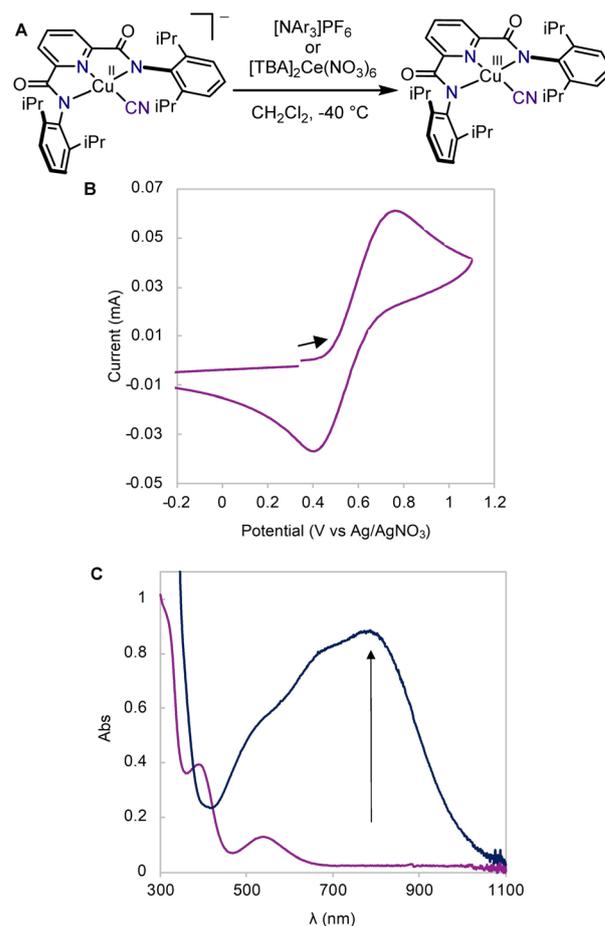

Fig. 1 (A) Synthesis of **LCu^{III}CN**. (B) Cyclic voltammogram of [TBA]**LCu^{II}CN** (3 mM in CH$_2$Cl$_2$ with 0.1 M [TBA]ClO$_4$ at 23°. (C) UV-vis spectra showing the formation of **LCu^{III}CN** (dark blue trace) by chemical oxidation of [TBA]**LCu^{II}CN** (purple trace) in CH$_2$Cl$_2$ at −40 °C.

oxidation of [TBA]**LCu^{II}CN** with variable temperature UV-vis spectroscopy. Treatment of [TBA]**LCu^{II}CN** with the triarylaminium radical cation, [NAr$_3$]PF$_6$ (Ar = 4-bromophenyl, $E_{1/2} = 0.70$)[47] at −40 °C in CH$_2$Cl$_2$ reveals the rapid formation of a new species with intense absorption at 790 nm ($\varepsilon = 8800$ M^{-1} cm^{-1}) (Fig. 1C). The observed optical features are very similar to other formal copper(III) species in the same ligand framework and are thus attributed to the **LCu^{III}CN** complex. Despite its highly oxidizing nature, the formal **LCu^{III}CN** complex is metastable in solution even at room temperature in CH$_2$Cl$_2$. **LCu^{III}CN** can also be generated by oxidation with [TBA]$_2$Ce(NO$_3$)$_6$ at −40 °C. When prepared from the Ce^{IV} oxidant, **LCu^{III}CN** exhibits lower thermal stability (slow decay at 0 °C), perhaps due to the extraction of the cyanide anion by the Lewis acidic Ce^{III} ion. Nonetheless, the Ce^{IV} route is better for large-scale preparation due to the ease of separation of **LCu^{III}CN** from the Ce^{III} byproduct. Extraction of **LCu^{III}CN** into diethyl ether led to its isolation as an analytically pure microcrystalline solid in 95% yield. The isolated solid **LCu^{III}CN** can be stored at −35 °C indefinitely.

Spectroscopic and structural characterization further confirms the formation of a formal copper(III) cyanide complex. The ^{1}H NMR spectrum of **LCu^{III}CN** in CD$_2$Cl$_2$ at room temperature exhibits

C1-N4 = 1.148(3) Å
Cu-C1 = 1.944(2) Å
Cu-N$_{avg}$ = 1.9874 Å

C1-N4 = 1.142(3) Å
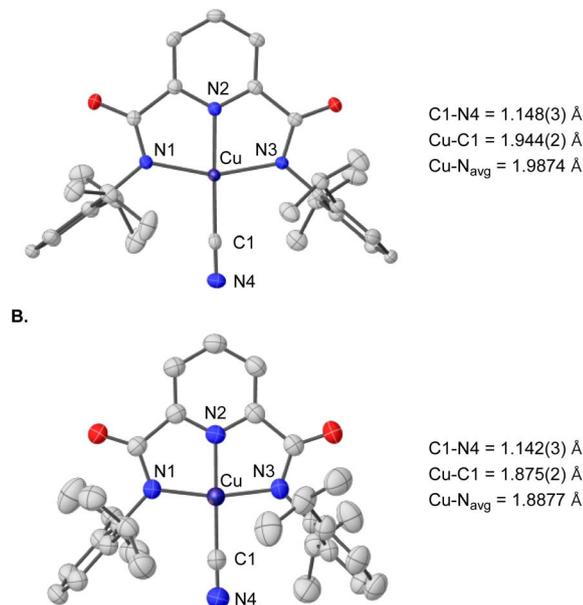Cu-C1 = 1.875(2) Å
Cu-N$_{avg}$ = 1.8877 Å

Fig. 2 Single-crystal X-ray diffraction structures and selected structural parameters of (A) [TBA]LCu^{II}CN and (B) LCu^{III}CN with thermal ellipsoids shown at 50% level of probability. Counterions, co-crystallized solvents, and hydrogen atoms are omitted for clarity.

sharp resonances within the 0–9 ppm range that account for all ligand protons (Fig. S4†). Furthermore, LCu^{III}CN is EPR silent at cryogenic and room temperatures (Fig. S6†). Collectively, the NMR and EPR studies suggest a diamagnetic ground state for LCu^{III}CN, similar to the analogous halide, hydroxo, and alkoxo complexes.[29,48] Infrared spectroscopy was used to gain further insight into the bonding between CN and the Cu center. Coordination of [TBA]CN to LCu^{II}MeCN shows a shift in the C≡N stretching frequency from 2055 cm^{-1} to 2141 cm^{-1}, indicating that binding to the Lewis acidic copper(II) strengthens the C≡N bond. Upon oxidation of [TBA]LCu^{II}CN to LCu^{III}CN, the C≡N stretching frequency shifts to 2164 cm^{-1} (Fig. S7†). We attribute the higher C≡N stretching frequency in LCu^{III}CN to the decreased π back-bonding resulting from the increase in Cu effective nuclear charge. Single-crystals of LCu^{III}CN were grown from vapor diffusion of pentane into a THF solution of LCu^{III}CN at −35 °C (Fig. 2B). The structure of LCu^{III}CN displays retention of the square planar
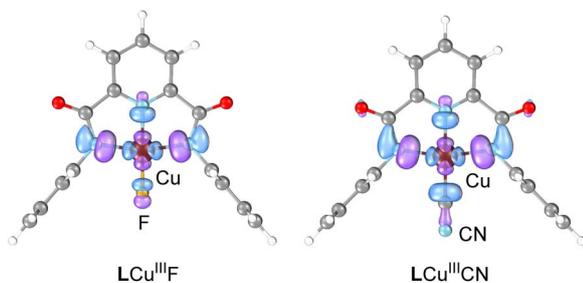
geometry with contraction of the copper–ligand bond distances by 0.07–0.1 Å compared to the copper(II) complex, in agreement with the higher effective nuclear charge of LCu^{III}CN. The C≡N bond length remains essentially the same, consistent with the minimal change in the C≡N stretching frequency upon oxidation. LCu^{III}CN is the first isolated and crystallographically characterized formal copper(III) complex bearing a cyanide and sp hybridized C donor ligand.

Multireference calculations with complete active space self-consistent field (CASSCF) and N-electron valence second-order perturbation theory (NEVPT2) were performed to compare the electronic structure of LCu^{III}CN and LCu^{III} halides. Similar to the halide analogs, LCu^{III}CN has a singlet ground state and multi-configurational electronic structure. The adiabatic singlet–triplet energy gap computed by NEVPT2 with 8 electrons in 8 active orbitals is 36.6 kcal mol^{-1} for LCu^{III}CN and 22.6 kcal mol^{-1} for LCu^{III}F. The most significant difference between the electronic structure of LCu^{III}CN and LCu^{III} halides is in the composition and occupation of the lowest unoccupied natural orbital (LUNO), which is the key orbital for both HAA and radical capture (RC). For both LCu^{III}F and LCu^{III}CN, the LUNO is comprised of the σ antibonding interactions between the Cu d$_{x^2-y^2}$ and ligand π orbitals (Fig. 3). However, while the LUNO of LCu^{III}F has orbital density equally distributed on either side of the fluorine atom, the LUNO of LCu^{III}CN is centered mainly on the C atom of CN, partly due to the π interactions between CN and Cu. In addition, the LCu^{III}CN LUNO has a lower occupation (0.14 e$^-$) than the LCu^{III}F LUNO (0.20 e$^-$), in agreement with the larger singlet–triplet gap of LCu^{III}CN.

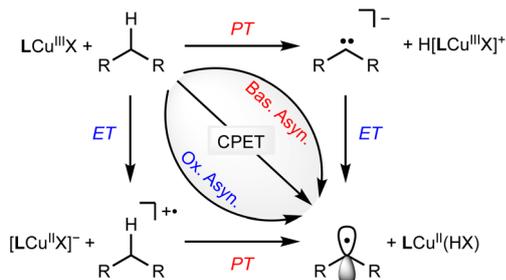## Hydrogen atom abstraction reactivity of LCu^{III}CN

The spectroscopic and structural resemblance of LCu^{III}CN to LCu^{III}F motivated us to expand the scope of Cu^{III}/Cu^{II}-promoted C–H functionalization. We began by studying the reaction between LCu^{III}CN and the hydrogen atom donor, 9,10-dihydroanthracene (DHA, C–H BDE 76.3 kcal mol^{-1}). The second-order rate constant of HAA with LCu^{III}CN is approximately three orders of magnitude lower than that of LCu^{III}F and five orders of magnitude lower than that of LCu^{III}OH (Fig. S12†). Monitoring the reaction between LCu^{III}CN and DHA at varying temperatures from 0 to 30 °C gave activation parameters $\Delta H^{\ddagger}$ = 9.4(1.6) kcal mol^{-1} and $\Delta S^{\ddagger}$ = −37(5) eu (Fig. S13†). The self-decay of the LCu^{III}CN complex at 30 °C is negligible (Fig. S14†). Notably, the enthalpy of activation is significantly disfavored for LCu^{III}CN compared to LCu^{III}F and

Fig. 3 Lowest unoccupied natural orbitals of LCu^{III}F and LCu^{III}CN from CASSCF calculation with 8 electrons in 8 active orbitals. Orbitals are shown at an isovalue of 0.05.

Table 1 Comparison of Eyring parameters for the reactions between DHA and LCu^{III}FG complexes

	$\Delta H^{\ddagger}$ (kcal mol^{-1})	$\Delta S^{\ddagger}$ (eu)	$\Delta G^{\ddagger c}$ (kcal mol^{-1})	Ref.
LCu^{III}CN[a]	9.4(1.6)	−37(5)	20	This work
LCu^{III}F[a]	3.8(2)	−43(1)	16	24
LCu^{III}OH[b]	5.1(1)	−31(3)	14	15

[a] Data collected in CH$_2$Cl$_2$. [b] Data collected in 1,2-difluorobenzene by Tolman et al. [c] Calculated at 20 °C.

Scheme 2 Possible mechanisms of PCET by $LCu^{III}FG$ complexes.

Fig. 5 Plot of $\log(k_{obs})$ versus (A) driving force of electron transfer $-\Delta G_{ET}$ ($R^2 = 0.893$), and (B) BDE ($R^2 = 0.2883$).

$LCu^{III}OH$ (Table 1), while the entropy of activation is comparable.[21,29]

The coupled movement of electron and proton during HAA has important implications on the kinetic barrier. The extent of proton/electron coupling in PCET reactions ranges from concerted proton electron transfer (CPET), in which the proton and electron are transferred in a single kinetic step, to stepwise electron transfer–proton transfer (ET–PT) or proton transfer–electron transfer (PT–ET, Scheme 2).[11,49,50] For example, it has been demonstrated that $LCu^{III}OH$ activates C–H bonds via a synchronous CPET reaction.[19–22] The mechanistic space between CPET and stepwise reactions is occupied by asynchronous CPET reactions, in which the proton and electron are transferred together, but with one leading the other (Scheme 2). Mid- to late-transition metal-oxo complexes are often highly basic and undergo C–H activation via basic asynchronous PCET, where the transition state exhibits predominant PT characters.[7,9,12,51,52] Tolman and Cramer et al. provide computational evidence that $LCu^{III}O_2CAr$ complexes activate C–H bonds through a rare oxidative asynchronous process with a transition state bearing ET character (Scheme 2).[12] The different dependence of k_{PCET} on thermodynamic factors of PCET (ΔG_{PT}°, ΔG_{ET}°, ΔG_{PCET}°) suggests that C–H activation selectivity can be tuned by the identity of the functional group in high-valent M–FG complexes.

To futher understand HAA by $LCu^{III}CN$, we examined the reactivity of $LCu^{III}CN$ with a series of H-atom donors. All reactions were monitored by UV-vis spectroscopy at 20 °C in CH_2Cl_2. Gas chromatography-mass spectrometry analysis of the reaction mixtures revealed the corresponding oxidized hydrocarbons, but no C–H cyanation products (see the ESI†). The pseudo-first-order
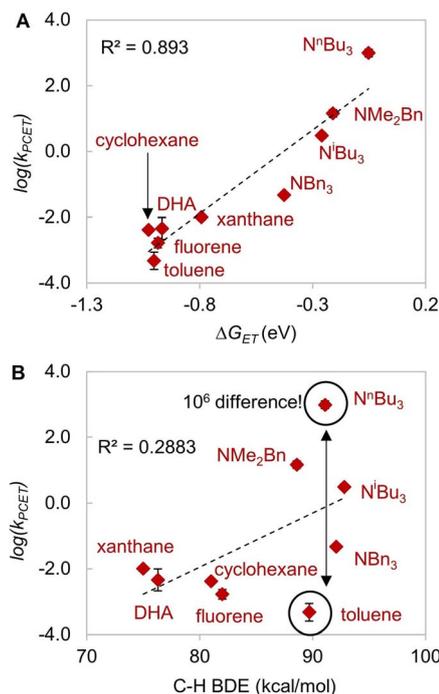
rate constants, k_{obs}, were plotted versus the BDE, pK_a, and E° of the C–H substrates (Fig. 4). The resulting plots show a linear correlation between HAA rates and C–H BDEs with an R^2 value of 0.91, supporting a concerted, homolytic C–H bond cleavage reaction (Fig. 5A). The Brønsted α value (Fig. 4A) obtained from this plot is 0.048, which is quite low for concerted CPET process,[53] indicating a high degree of transition state asymmetry.[54] The correlations of k_{obs} with E° and pK_a of the C–H substrates are poor with R^2 values of 0.39 and 0.09, respectively (Fig. 4B and C). We also attempted to correlate the rates of C–H activation with the driving forces of ΔG_{PCET}, ΔG_{PT}, and ΔG_{ET} using semiempirical models based on the work of Anderson and Borovik (see the ESI, Fig. S75 and S76†).[52,55] The results show a predominant contribution from ΔG_{PCET} with minor influence from ΔG_{ET}, further supporting concerted C–H activation with benzylic and allylic C–H substrates.
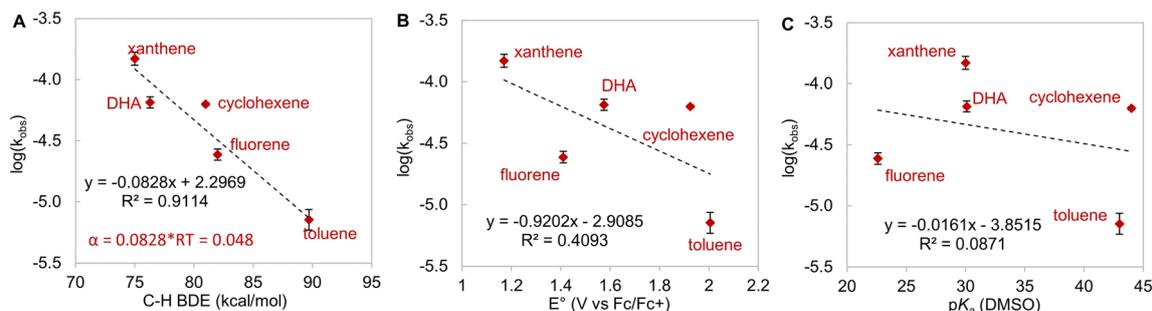

Fig. 4 Plot of $\log(k_{obs})$ versus (A) C–H bond dissociation energy ($R^2 = 0.91$), (B) pK_a ($R^2 = 0.41$) and (C) E_{ox} ($R^2 = 0.09$) of the substrates for the reaction of $LCu^{III}CN$ with 100 eq. of hydrocarbon C−H substrates.

Table 2 BDE of substrates, ET driving force ($-\Delta G_{ET}$), and asynchronicity factors (η), the second-order rate constant (k_{PCET} or k_{ET}) for the oxidation of C–H substrates with $\mathbf{LCu^{III}CN}$ in DCM at 20 °C

Substrate	C–H BDE	η (V)	$-\Delta G_{ET}$ (eV)	k_{PCET} or k_{ET} (M^{-1} s^{-1})
Fluorene	82.0	0.076	−0.985	$1.7(6) \times 10^{-3}$
DHA	76.3	0.146	−0.967	$5(5) \times 10^{-3}$
Toluene	89.7	0.441	−1.00	$5(4) \times 10^{-4}$
Xanthene	75.0	0.470	−0.792	$1.0(2) \times 10^{-2}$
Cyclohexene	81	—	−1.03	$4.1(6) \times 10^{-3}$
NBn$_3$	92.1	1.22	−0.427	$4.7(4) \times 10^{-2}$
N^{i}Bu$_3$	92.8	1.34	−0.259	3.1(6)
NMe$_2$Bn	88.6	1.34	−0.210	15(4)
N^{n}Bu$_3$	91.1	1.41	−0.052	$10(3) \times 10^2$

Table 3 Amine α-C–H cyanation reactivity of $\mathbf{LCu^{III}CN}$

Reactivity of LCu^{III}CN with amines

The lack of C–H cyanation reactivity toward benzylic and allylic substrates by $\mathbf{LCu^{III}CN}$ prompted us to consider other strategies to reduce the barrier of HAA/PCET. A recent study by Srnec *et al.* suggests that more asynchronous PCET processes, as characterized by a larger $|\eta|$ value, give rise to a lower activation free energy and faster PCET.[7] The η value can be calculated by considering the thermodynamics of ET and PT:[52]

$$\eta = 2^{-1/2} \times (\Delta E^{\circ} - RT/F \times \ln(10) \times \Delta pK_{a,ox}).$$

where

$$\Delta E^{\circ} = E^{\circ}_{LCuCN} - E^{\circ}_{substrate}.$$

$$\Delta pK_{a,ox} = pK_a^{LCuCN,ox} - pK_a^{substrate,ox}.$$

The $\mathbf{LCu^{III}CN}$ complex is unstable toward protonation, preventing the experimental determination of pK_a. Nonetheless, based on the reactivity of $\mathbf{LCu^{III}CN}$ with various acids, we estimated the pK_a of $\mathbf{LCu^{III}CN}/[\mathbf{LCu^{III}CN}]H^+$ to be less than 4.4 (see the ESI†). As shown in the equations above, the absolute pK_a value of $\mathbf{LCu^{III}CN}/[\mathbf{LCu^{III}CN}]H^+$ ($pK_a^{LCuCN,ox}$) does not change the difference in η value between substrates, since $pK_a^{LCuCN,ox}$ is a common term for all the η calculation. Combining the estimated pK_a with the experimentally determined $E_{1/2}$ of $\mathbf{LCu^{III}CN}$ in DMSO (0.295 V *vs.* Fc/Fc$^+$), we have found that the η values of C–H substrates are generally positive, indicating oxidative asynchronous CPET or ET–PT (Table 2).

Since C–H activation by $\mathbf{LCu^{III}CN}$ is biased for oxidative asynchronous processes, substrates that exhibit even more positive η values (more oxidative asynchronicity) than benzylic/allylic C–H substrates for HAA by $\mathbf{LCu^{III}CN}$ should have a lower kinetic barrier of HAA/PCET. Therefore, we consider amines as possible substrates due to their mild oxidation potentials ($E^{\circ} = \sim0.4$–1 V *vs.* Fc/Fc$^+$ in MeCN) and low acidities ($pK_a \geq 40$).[56,57] Indeed, the η values of amines (1.22–1.41 V) are substantially higher than those of benzylic and allylic substrates (0.076–0.470 V). The comparison between trialkylamines and toluene is noteworthy as they have similar bond dissociation enthalpies (BDEs, 89–93 kcal mol^{-1} (ref.
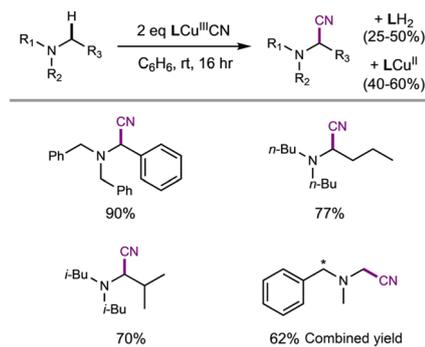
46) and 89.7 kcal mol^{-1}) but very different η values ($\eta_{tributylamine} = 1.41$ V; $\eta_{toluene} = 0.441$ V).

According to Srnec's theory, $\mathbf{LCu^{III}CN}$ is expected to activate trialkylamines at a much faster rate because CPET with tributylamine is more asynchronous (larger $|\eta|$). Indeed, we found that $\mathbf{LCu^{III}CN}$ activates trialkylamines faster than toluene by 10^3 to 10^6-fold (Table 2)! While the plot of log(k_{PCET}) *versus* BDEs with C–H substrates shows good correlation with benzylic and allylic substrates (Fig. 4A), the R^2 value drops down to 0.2883 if amine substrates are included in the plot (Fig. 5A). In contrast, the plot of log(k_{PCET}) *versus* the driving force of electron transfer ($-\Delta G_{ET}$) now shows a good correlation with $R^2 = 0.893$ (Fig. 5B), suggesting that electron transfer is the determining factor for the rate of PCET. The PCET rate of N^{n}Bu$_3$ appears to be an outlier (Fig. 5B), potentially due to a mechanism crossover from oxidative asynchronous PCET to stepwise ET–PT. It is possible that the amine substrates lie on a different line due to stepwise ET–PT. Similar phenomena have been observed by Kojima[13,14] and Fukuzumi.[15]

Additionally, $\mathbf{LCu^{III}CN}$ not only activates α-amino C–H bonds efficiently but also furnishes the amine C–H cyanation products. Treatment of trialkylamines with two equivalents of $\mathbf{LCu^{III}CN}$ in benzene at room temperature affords the corresponding α-aminonitrile products in 62–90% yield (Table 3). The reaction of $\mathbf{LCu^{III}CN}$ with *N,N*-dimethyl-1-phenylmethanamine furnishes a mixture of nitrile products at the aliphatic and benzylic positions in a combined 62% yield. To evaluate the role of Cu, control experiments were performed by treating amine substrates with two equivalents of the one-electron oxidant [NAr$^{Br}_3$]$^+$ in the presence of TBACN. The cyanation products were also observed in 10–55% yield (Fig. S54–S57†), indicating that an ET-initiated cyanation is possible.[58] The higher yields by $\mathbf{LCu^{III}CN}$ can be attributed to the fact that $\mathbf{LCu^{III}CN}$ can serve as both the oxidant and the source of cyanide.

Following the stoichiometric C–H cyanation reactions, we observed varying amounts of protonated ligand $\mathbf{LH_2}$ (25–50%) by ^{1}H NMR, indicating that the dianionic ligand $\mathbf{L^{2-}}$ serves as the terminal proton acceptor. Furthermore, the copper(II) byproduct can be recovered as $\mathbf{LCu^{II}MeCN}$ in 40–60% spectroscopic yields according to UV-vis and EPR analysis (see the ESI†). This dual C–H activation/radical "rebound" type of reactivity has only been observed with $\mathbf{LCu^{III}F}$ (ref. [29]) and $\mathbf{LCu^{III}NO_2}$.[23] However, the

narrow substrate scope, as well as the use of stoichiometric amount of $\textbf{LCu}^{\text{III}}\text{CN}$, limits the use of this method compared to state-of-the-art C–H cyanation protocols.[58–60]

Conclusion

In summary, we report the synthesis and characterization of the first formal copper(III) cyanide complex. Despite the similar spectroscopic properties of $\textbf{LCu}^{\text{III}}\text{F}$ and $\textbf{LCu}^{\text{III}}\text{CN}$, their reactivities stand in stark contrast. While $\textbf{LCu}^{\text{III}}\text{F}$ is quite reactive towards benzylic and allylic C–H bonds, HAA by $\textbf{LCu}^{\text{III}}\text{CN}$ is approximately 10^3 times slower. A very striking result of our study is that the rate of C–H activation with $\textbf{LCu}^{\text{III}}\text{CN}$ can be increased by 10^3–10^7-fold by polarity matching, as characterized by the asynchronicity factor η. This observation is consistent with the prediction by Srnec that asynchronous processes have smaller activation barriers than synchronous processes with the same driving force $\Delta G^{\circ}_{\text{PCET}}$. We further demonstrate that $\textbf{LCu}^{\text{III}}\text{CN}$ is capable of the C–H cyanation of tertiary amines. The reaction proceeds through 2 : 1 stoichiometry with $\textbf{LCu}^{\text{III}}\text{CN}$ performing both HAA/PCET and CN group transfer.

Polarity matching strategies have been demonstrated in sp³ C–H activation with organic radicals to facilitate selectivity beyond the conventional bond dissociation energy model.[61–63] Herein, we show that a similar strategy can be applied to metal-based oxidants. Pairing the oxidative ability of $\textbf{LCu}^{\text{III}}\text{CN}$ with the oxidizable nature of amines allows the development of HAA/PCET processes not dictated by the thermodynamic driving force of the reaction itself. While it is still early to conclude whether high asynchronicity factors $|\eta|$ generally lead to faster HAA rates, the success of this model in our case is part of a growing number of studies that suggest the (im)balance between $\Delta G^{\circ}_{\text{PT}}$ and $\Delta G^{\circ}_{\text{ET}}$, considered in the form of asynchronicity factor η (the difference between $\Delta G^{\circ}_{\text{PT}}$ and $\Delta G^{\circ}_{\text{ET}}$) or empirical models, plays a critical role in understanding the rates of HAA.[9,52,53,55] The comparison of $\textbf{LCu}^{\text{III}}\text{CN}$ and $\textbf{LCu}^{\text{III}}$ halides shows that changing the functional group bound to the copper(III) center opens new avenues for accessing distinct mechanistic pathways. Studies to further generalize the copper(II)/(III)-mediated C–H functionalization with other functional groups are ongoing in our laboratory.

Data availability

All other data supporting the findings of this study are available in the ESI.†

Author contributions

Conceptualization: JKB, AYS, SZ; methodology: JKB, MR, IMM; investigation: JKB, MR, LMZ, IMM, ADC, CEM; writing – original draft: JKB, AYS, SZ; writing – review & editing: MR, AYS, SZ; funding acquisition: SZ, AYS.

Conflicts of interest

The authors have no conflicts to declare.

Acknowledgements

References

1 J. Rittle and M. T. Green, *Science*, 2010, **330**, 933–937.

2 X. Huang and J. T. Groves, *J. Biol. Inorg Chem.*, 2017, **22**, 185–207.

3 A. R. McDonald and L. Que, *Coord. Chem. Rev.*, 2013, **257**, 414–428.

4 A. S. Borovik, *Chem. Soc. Rev.*, 2011, **40**, 1870–1874.

5 M. H. V Huynh and T. J. Meyer, *Chem. Rev.*, 2007, **107**, 5004–5064.

6 J. J. Warren, T. A. Tronic and J. M. Mayer, *Chem. Rev.*, 2010, **110**, 6961–7001.

7 D. Bím, M. Maldonado-Domínguez, L. Rulísek and M. Srnec, *Proc. Natl. Acad. Sci. U. S. A.*, 2018, **115**, E10287–E10294.

8 R. G. Agarwal, S. C. Coste, B. D. Groff, A. M. Heuer, H. Noh, G. A. Parada, C. F. Wise, E. M. Nichols, J. J. Warren and J. M. Mayer, *Chem. Rev.*, 2022, **122**, 1–49.

9 M. K. Goetz and J. S. Anderson, *J. Am. Chem. Soc.*, 2019, **141**, 4051–4062.

10 B. S. K., Y. Meng-Yin, P. T. H., G. M. T. and B. A. S., *Proc. Natl. Acad. Sci. U. S. A.*, 2021, **118**, e2108648118.

11 T. H. Parsell, M. Y. Yang and A. S. Borovik, *J. Am. Chem. Soc.*, 2009, **131**, 2762–2763.

12 M. Mandal, C. E. Elwell, C. J. Bouchey, T. J. Zerk, W. B. Tolman and C. J. Cramer, *J. Am. Chem. Soc.*, 2019, **141**, 17236–17244.

13 S. Miyazaki, T. Kojima, J. M. Mayer and S. Fukuzumi, *J. Am. Chem. Soc.*, 2009, **131**, 11615–11624.

14 H. Kotani, S. Kaida, T. Ishizuka, M. Sakaguchi, T. Ogura, Y. Shiota, K. Yoshizawa and T. Kojima, *Chem. Sci.*, 2015, **6**, 945–955.

15 Y. Morimoto, J. Park, T. Suenobu, Y.-M. Lee, W. Nam and S. Fukuzumi, *Inorg. Chem.*, 2012, **51**, 10025–10036.

16 A. Gunay and K. H. Theopold, *Chem. Rev.*, 2010, **110**, 1060–1081.

17 W. Liu and J. T. Groves, *Acc. Chem. Res.*, 2015, **48**, 1727–1735.

18 M. Puri, A. N. Biswas, R. Fan, Y. Guo and L. Que, *J. Am. Chem. Soc.*, 2016, **138**, 2484–2487.

19 P. J. Donoghue, J. Tehranchi, C. J. Cramer, R. Sarangi, E. I. Solomon and W. B. Tolman, *J. Am. Chem. Soc.*, 2011, **133**, 17602–17605.

20 D. Dhar and W. B. Tolman, *J. Am. Chem. Soc.*, 2015, **137**, 1322–1329.

21 D. Dhar, G. M. Yee, A. D. Spaeth, D. W. Boyce, H. Zhang, B. Dereli, C. J. Cramer and W. B. Tolman, *J. Am. Chem. Soc.*, 2016, **138**, 356–368.

22 C. E. Elwell, M. Mandal, C. J. Bouchey, L. Que, C. J. Cramer and W. B. Tolman, *Inorg. Chem.*, 2019, **58**, 15872–15879.

23 C. J. Bouchey and W. B. Tolman, *Inorg. Chem.*, 2022, **61**, 2662–2668.

24 P. Pirovano, E. R. Farquhar, M. Swart and A. R. McDonald, *J. Am. Chem. Soc.*, 2016, **138**, 14362–14370.

25 P. Mondal, P. Pirovano, A. Das, E. R. Farquhar and A. R. McDonald, *J. Am. Chem. Soc.*, 2018, **140**, 1834–1841.

26 D. Unjaroen, R. Gericke, M. Lovisari, D. Nelis, P. Mondal, P. Pirovano, B. Twamley, E. R. Farquhar and A. R. Mcdonald, *Inorg. Chem.*, 2019, **58**, 16838–16848.

27 P. Mondal, M. Lovisari, B. Twamley and A. R. McDonald, *Angew. Chem., Int. Ed.*, 2020, **59**, 13044–13050.

28 C. Panda, L. M. Doyle, R. Gericke and A. R. McDonald, *Angew. Chem., Int. Ed.*, 2021, **60**, 26281–26286.

29 J. K. Bower, A. D. Cypcar, B. Henriquez, S. C. E. Stieber and S. Zhang, *J. Am. Chem. Soc.*, 2020, **142**, 8514–8521.

30 T. Corona, A. Draksharapu, S. K. Padamati, I. Gamba, V. Martin-Diaconescu, F. Acuna-Parés, W. R. Browne and A. Company, *J. Am. Chem. Soc.*, 2016, **138**, 12987–12996.

31 K. J. Fisher, M. L. Feuer, H. M. C. Lant, B. Q. Mercado, R. H. Crabtree and G. W. Brudvig, *Chem. Sci.*, 2020, **11**, 1683–1690.

32 Y. M. Kwon, Y. Lee, G. E. Evenson, T. A. Jackson and D. Wang, *J. Am. Chem. Soc.*, 2020, **142**, 13435–13441.

33 D. Enders and J. P. Shilvock, *Chem. Soc. Rev.*, 2000, **29**, 359–373.

34 T. S. Ratani, S. Bachman, G. C. Fu and J. C. Peters, *J. Am. Chem. Soc.*, 2015, **137**, 13902–13907.

35 N. Miwa, C. Tanaka, S. Ishida, G. Hirata, J. Song, T. Torigoe, Y. Kuninobu and T. Nishikata, *J. Am. Chem. Soc.*, 2020, **142**, 1692–1697.

36 K. Kim and S. H. Hong, *Adv. Synth. Catal.*, 2017, **359**, 2345–2351.

37 W. Zhang, F. Wang, S. D. McCann, D. Wang, P. Chen, S. S. Stahl and G. Liu, *Science*, 2016, **353**, 1014–1018.

38 Z. Zhang, X. Zhang and D. A. Nagib, *Chem*, 2019, **5**, 3127–3134.

39 C. Y. Wang, Z. Y. Qin, Y. L. Huang, R. X. Jin, Q. Lan and X. S. Wang, *iScience*, 2019, **21**, 490–498.

40 R. Lu, T. Yang, X. Chen, W. Fan, P. Chen, Z. Lin and G. Liu, *J. Am. Chem. Soc.*, 2021, **143**, 14451–14457.

41 P. F. Zhu, Y. X. Si and S. L. Zhang, *Org. Biomol. Chem.*, 2020, **18**, 9216–9220.

42 J. Li, Z. Zhang, L. Wu, W. Zhang, P. Chen, Z. Lin and G. Liu, *Nature*, 2019, **574**, 516–521.

43 H. Chen, W. Jin and S. Yu, *Org. Lett.*, 2020, **22**, 5910–5914.

44 D. Wang, N. Zhu, P. Chen, Z. Lin and G. Liu, *J. Am. Chem. Soc.*, 2017, **139**, 15632–15635.

45 F. D. Lu, D. Liu, L. Zhu, L. Q. Lu, Q. Yang, Q. Q. Zhou, Y. Wei, Y. Lan and W. J. Xiao, *J. Am. Chem. Soc.*, 2019, **141**, 6167–6172.

46 J. Lalevée, X. Allonas and J. P. Fouassier, *J. Am. Chem. Soc.*, 2002, **124**, 9613–9621.

47 N. G. Connelly and W. E. Geiger, *Chem. Rev.*, 1996, **96**, 877–910.

48 V. M. Krishnan, D. Y. Shopov, C. J. Bouchey, W. D. Bailey, R. Parveen, B. Vlaisavljevich and W. B. Tolman, *J. Am. Chem. Soc.*, 2021, **143**, 3295–3299.

49 M. Asaka and H. Fujii, *J. Am. Chem. Soc.*, 2016, **138**, 8048–8051.

50 M. J. Zdilla, J. L. Dexheimer and M. M. Abu-Omar, *J. Am. Chem. Soc.*, 2007, **129**, 11505–11511.

51 D. Usharani, D. C. Lacy, A. S. Borovik and S. Shaik, *J. Am. Chem. Soc.*, 2013, **135**, 17090–17104.

52 S. K. Barman, M. Y. Yang, T. H. Parsell, M. T. Green and A. S. Borovik, *Proc. Natl. Acad. Sci. U. S. A.*, 2021, **118**, e2108648118.

53 J. W. Darcy, S. S. Kolmar and J. M. Mayer, *J. Am. Chem. Soc.*, 2019, **141**, 10777–10787.

54 G. Qiu and R. R. Knowles, *J. Am. Chem. Soc.*, 2019, **141**, 2721–2730.

55 J. E. Schneider, M. K. Goetz and J. S. Anderson, *Chem. Sci.*, 2021, **12**, 4173–4183.

56 Y. L. Chow, S. F. Nelsen and D. H. Rosenblatt, *Chem. Rev.*, 1978, **78**, 243–274.

57 S. V. Kessar and P. Singh, *Chem. Rev.*, 1997, **97**, 721–737.

58 A. J. J. Lennox, S. L. Goes, M. P. Webster, H. F. Koolman, S. W. Djuric and S. S. Stahl, *J. Am. Chem. Soc.*, 2018, **140**, 11227–11231.

59 D. H. R. Barton, A. Billion and J. Boivin, *Tetrahedron Lett.*, 1985, **26**, 1229–1232.

60 D. B. Ushakov, K. Gilmore, D. Kopetzki, D. T. McQuade and P. H. Seeberger, *Angew. Chem., Int. Ed.*, 2014, **53**, 557–561.

61 J. M. Tedder, *Angew. Chem., Int. Ed. Engl.*, 1982, **21**, 401–410.

62 B. P. Roberts, *Chem. Soc. Rev.*, 1999, **28**, 25–35.

63 C. Le, Y. Liang, R. W. Evans, X. Li and D. W. C. MacMillan, *Nature*, 2017, **547**, 79–83.